Development of a Lycopodium powder-based superhydrophobic nanofiber membrane suitable for desalination

M. Essalhi[1], M. Khayet[2,3,*], A. B. Yavuz[4], L. R. de la Rosa[2], M.C. García-Payo[2], N. Tavajohi[1,*]

[1] Department of Chemistry, Umeå University, 90187, Umeå, Sweden.

[2] Department of Structure of Matter, Thermal Physics and Electronics, Faculty of Physics, University Complutense of Madrid, Avda. Complutense s/n, 28040, Madrid, Spain.

[3] Madrid Institute for Advanced Studies of Water (IMDEA Water Institute), Calle Punto Net Nº 4, 28805, Alcalá de Henares, Madrid, Spain.

[4] Department of Chemistry, Agri Ibrahim Cecen University, Agri, Turkey.

* Corresponding authors:

khayetm@fis.ucm.es (M. Khayet) Tel. +34-3945185

naser.tavajohi@umu.se (N. Tavajohi) Tel. +46-907866061

Abstract

A biobased, green, inexpensive additive, Lycopodium particles, which are spores of the "*Lycopodium clavatum*" plant, were incorporated in the poly(vinylidene fluoride) PVDF electrospun nanofiber membranes (ENMs) for desalination by direct contact membrane distillation (DCMD). Superhydrophobic ENMs were prepared using this additive (PVDF-ENMs-Lyc). Thanks to their morphological structure and their prominent surface superhydrophobicity (anti-wetting) character, the resulting PVDF-ENMs-Lyc exhibited an improved liquid entry pressure (*LEP*), a high void volume fraction (greater than 87.2%), a good salt rejection factor (greater than 99.93%) and a reasonably high permeate flux (greater than 51.76 $kg \cdot m^{-2} \cdot h^{-1}$) at 80 ºC, which are of great practical importance for water desalination by DCMD. The optimum membrane prepared with 3 wt% Lycopodium in the dope solution demonstrated a stable permeate flux of 52.4 ± 0.6 $kg \cdot m^{-2} \cdot h^{-1}$ with an electrical conductivity around 4.76 ± 0.46 µS/cm (NaCl rejection factor of 99.998 ± 0.036%) during 25 h DCMD desalination experiment using 35 g/L NaCl aqueous solution (similar to seawater concentration). The presented results pave the way for superhydrophobic nanofibrous membrane engineering suitable for membrane contactors by electrospinning in a single step without surfactants, organic additives, or chemical post-treatments, just by the incorporation of a green additive like Lycopodium powder.

Keywords

Electrospinning; Nanofibrous electrospun membrane; Lycopodium powder; Membrane distillation; Polyvinylidene fluoride; Green additive; Superhydrophobicity.

Nomenclature

Abbreviations

CFF	Filter flow distribution
DCMD	Direct contact membrane distillation
DMAC	N, N-dimethylacetamide
ENMs	Electrospun nanofibrous membranes
FESEM	Field emission scanning electron microscope
IPA	Isopropyl alcohol
LEP	Liquid entry pressure (10^3 Pa)
MD	Membrane Distillation
NaCl	Sodium chloride
PVDF	Polyvinylidene fluoride
PVDF-ENM-Lyc-x	PVDF nanofibrous membrane containing x wt% Lycopodium

Symbols

μ_p	Viscosity (Pa·s)
C_f	NaCl concentration in the feed (g/L)
C_p	NaCl concentration in the permeate (g/L)
d_f	Fiber diameters (nm)
d_i	Mean inter-fiber space size (μm)
J_w	Water vapor permeate flux (kg⁄m^2·h)
T	DCMD operating time (h)
T_f	Feed temperature (ºC)
T_p	Permeate temperature (ºC)
W	Circulation stirring rate of the feed and the permeate liquid solutions (rpm)
A	Salt rejection factor (%)
Δ	Thickness (μm)
E	Void volume fraction (%)
θ	Contact angle
Ω_p	Permeate electrical conductivity (μS/cm)
$\Omega_{polymer}$	Electrical conductivity of polymer solution ((μS/cm)
$\mu_{polymer}$	Viscosity of polymer solution (Pa·s)
$\sigma_{polymer}$	Surface tension of polymer solution (mN/m)

1. Introduction

Globally, natural water resources are diminishing with an alarming rhythm caused by worldwide exponential population growth, accelerated urbanization, and human exploitation, thus decreasing the availability of clean water dramatically. Consequently, membrane separation technology has become a highly pursued strategy for desalination and potable water production [1]. Within the broad range of existing desalination and water purification technologies, reverse osmosis (RO) is the leading one. However, it remains subject to high operational hydrostatic pressures and subsequent energy consumption, especially for the treatment of high saline waters [2, 3]. Alternatively, the non-isothermal separation technology of emerging interest membrane distillation (MD), based on the use of hydrophobic microporous membranes, can produce distilled water from high saline aqueous solutions up to their saturation, including RO brines, as it is not limited by the osmotic pressure of the feed solution [4]. One of the advantages of MD is its high water recovery, excellent quality of the produced water, and low operating hydrostatic pressure [5]. The MD performance, particularly the permeate flux, is determined mainly by the vapor pressure gradient induced by the operating temperature difference, which established at both sides of the membrane kept at atmospheric pressure [6-8].

Several methods have been adopted to prepare membranes suitable for MD, including interfacial reactions, sol-gel processes, extrusion, etching, stretching, and polymer phase separation [9, 10]. However, most proposed membranes show unsatisfactory permeate fluxes caused by either low porosity, limited pore connectivity, membrane fouling/scaling propensity, or pore wetting, reducing therefore their lifetime [2]. Therefore, developing robust hydrophobic porous membranes with high porosity and pore interconnectivity is one of the hot topics in MD membrane engineering.

The simple, inexpensive, and cost-effective electrospinning technique has evolved into a state-of-the-art method for developing electrospun nanofibrous membranes (ENMs) using a wide range of different types of materials with a controlled thickness, tailored cross-section (i.e., single or multilayered; tight or loosed web) and different nanofiber diameters among others [11]. Having a series of outstanding inherent properties, ENMs play a pivotal position within several water treatment areas because of their high specific surface area, high surface-to-mass ratio, superior interconnected porosity (void volume fraction), mechanical robustness, high water permeability, high rejection of non-volatile solutes from water, low heat transfer by conduction (i.e., high thermal efficiency), good fouling resistance, and controllable wettability [12]. However, incorporating new additives to ENMs associated with improving their hydrophobicity without altering their internal properties remains one of the challenges to be solved.

Polyvinylidene fluoride (PVDF) and PVDF derivatives have been considered mainly for preparing ENMs for MD due to their intrinsic hydrophobicity. Yet, such ENMs still suffered from the unstable salt rejection property due to the low liquid entry pressure (*LEP*) induced by the relatively large fiber diameter and interfiber size of the ENMs [11, 13, 14]. This problem was addressed by improving the membrane surface hydrophobicity to produce superhydrophobic ENMs [15-17] and/or using hot-pressing post-treatments of the prepared ENMs [18-22]. For instance, incorporating additives, mainly nanomaterials, into electrospun membranes has been found to improve the membrane characteristics, such as its robustness, hydrophobicity, antifouling, and wetting properties [23-25]. The most commonly reported additives used to prepare MD ENMs include silica nanoparticles (SiNP) [26-29], fluorinated zinc oxide (ZnO) nanoparticles [30, 31], alumina nanoparticles, TiO_2 nanoparticles [32-34], clay nanoparticles [35, 36], graphene [37], carbon nanotubes (CNTs) [38-41], graphene oxide [39, 42], and other fluorinated materials [11, 43, 44]. As can be seen, both organic and inorganic

additives have been considered to improve the MD characteristics of ENMs [44-47]. However, using green additives to form mixed matrix membrane structure has been somehow overlooked in the past years.

Lycopodium, a fine yellow powder derived from the spores of the plant *Lycopodium clavatum*, exhibits a tremendous hydrophobic character [48-50]. Lycopodium's superhydrophobic character dates back to 1907 when H. Ollivier recorded contact angles of almost 180° on surfaces coated with soot, arsenic trioxide, and Lycopodium powder [51]. However, until the mid-1930s, this phenomenon started to gain considerable attention due to the first principles of superhydrophobicity outlined by Wenzel [52] and Cassie [53]. Lycopodium particles have been used for various purposes, including the increase of the polyethylene film hydrophobicity by stamping it on polyethylene surfaces [54], for liquid marble fabrication [55], for sorption of heavy metal ions from aqueous solution [56], as sole emulsifiers of oil and water mixtures [57], for use as biosorbent microcapsules to improve the magnetic removal of heavy metals or humic acid (HA) from different aqueous media [58], and to enhance drug delivery [59-61]. In the present research study, it is the first time that this green additive is used in MD membrane engineering. PVDF ENMs were prepared by electrospinning for desalination by DCMD. The effects of Lycopodium concentration on the ENMs´ surface morphology, surface wettability, structural characteristics, and DCMD performance were investigated.

2. Materials used, ENM preparation and characterization

Polyvinylidene fluoride (PVDF) polymer (M_w = 275,000 g/mol), N, N-dimethylacetamide (DMAc), acetone, POREFIL125 (surface tension 16 mN/m, Porometer), isopropyl alcohol (IPA), sodium chloride (NaCl, Panreac) and Lycopodium powder were purchased from Sigma-Aldrich Chemical Co. All chemicals used were of analytical grade and were used as received.

To obtain an homogeneous dispersion for the preparation of ENMs, a certain amount of Lycopodium powder was added to the DMAc/acetone solvent mixture (80/20 wt%) and then sonicated for 3 h using an ultrasonic bath (Fisher Scientific FB15047). Simultaneously, the PVDF was completely dissolved at 45°C in the DMAc/acetone solvent mixture (80/20 wt%). Subsequently, the PVDF solution was mixed with the Lycopodium dispersion for 5 h at 45°C using a magnetic stirrer (IKA, RCT basic) to obtain a homogeneous electrospinning solution. The prepared solution was then sonicated for an additional 3 h and subsequently degassed at room temperature overnight. The polymer concentration was 25 wt%, and the amount of Lycopodium was 0.25, 0.5, 1, 2, and 3 wt% in the electrospinning solution. For the sake of comparison, we prepared a reference electrospinning solution of PVDF (25 wt%) without Lycopodium.

For ENMS preparation, a glass syringe (Nikepal, 20 mL) connected to a syringe pump (KD Scientific, model KD.S-200-CE) was filled with 10 mL polymeric solution and turned on at a rate of 1.25 mL/hr. To ensure the flow of the polymeric solution from the syringe to the stainless-steel needle tip (Hamilton Company; inner/outer diameter 0.6/0.9 mm), a 50 cm Teflon tube was used. A positive DC voltage of 24 kV using a DC electric voltage source (Iseg; model T1CP 300 304P; 1 × 30 kV / 0.3 mA) was applied to the solution polymer solution, causing nanofibers formation. The distance between the needle tip and the grounded copper metallic collector covered with aluminum foil was 27.5 cm. The electrospinning time of each

ENM was kept at 90 min. The electrospinning temperature was 22.0 ± 1.5 °C, and the relative humidity was 28.9 ± 2.5%. All ENMs prepared in this study were subjected to a thermal post-treatment in a vacuum oven at 180 °C for 30 min to remove any residual solvent.

The electrical conductivity (Ω_p), viscosity (μ_p), and surface tension (σ_p) of the polymer solutions were measured with a conductivity meter (CyberScan CON11 Conductivity/TDS/°C, Eutech Instruments) equipped with a conductivity electrode (EC-CONSEN91W/35608-50), a digital viscometer (Brookfield, DV-I+) equipped with stainless steel spindles (LV1, LV2, LV3, and LV4) connected to a thermostat (Model HETO 21-DT-1, Rego SA), and an Optical Contact Angle Meter (CAM 200) employing pendant drop shape analysis, a stainless steel needle with an outer diameter of 1.827 mm, and a constant drop volume (12.5 ± 0.5 μL), respectively. All measurements were conducted at an average temperature of 22.5 °C. For each polymer solution, we report the average value together with its standard deviation derived from at least five measurements. The obtained values of Ω_p, μ_p, and σ_p are listed in Table 1.

Table 1. Electrical conductivity ($\Omega_{polymer}$), viscosity ($\mu_{polymer}$), and surface tension ($\sigma_{polymer}$) of the dope solutions (PVDF/Lycopodium/DMAc/acetone) used to prepare the ENMs.

Lycopodium (wt%)	$\boldsymbol{\Omega_{polymer}}$ **(μS/cm)**	$\boldsymbol{\mu_{polymer}}$ **(Pa·s)**	$\boldsymbol{\sigma_{polymer}}$ **(mN/m)**
0.00	08.96 ± 2.73	6.02 ± 0.08	31.23 ± 0.11
0.25	09.73 ± 2.13	6.83 ± 0.44	31.67 ± 0.25
0.50	10.25 ± 1.03	8.32 ± 0.83	32.41 ± 0.32
1.00	10.88 ± 0.54	11.44 ± 0.13	34.03 ± 0.41
2.00	11.05 ± 0.12	13.32 ± 1.22	34.93 ± 0.53
3.00	11.67 ± 0.21	15.12 ± 1.83	36.01 ± 0.41

To study the morphological characteristics of the prepared ENMs, field emission scanning electron microscopy (FESEM, JEOL model JSM-6335F) was employed to examine the ENMs surface after coating with a thin layer of gold of about 5 nm by an evaporator (EMITECH K550 X) at 25 mA for 1 minute. To analyze the SEM images of the ENM surface

and determine the nanofiber diameters (d_f) and their distributions, the UTHSCSA ImageTool 3.0 program was used. For each ENM, the average diameters together with their standard deviations were reported based on the diameters of a total number of 100 nanofibers and considering at least three different images at the same magnification.

The hydrophobic character of the prepared ENMs was analyzed by measuring the water contact angle (θ) of the surface of each sample. A computerized optical contact angle meter (CAM 200) equipped with a CCD camera and a stainless-steel needle together with the image analysis software (Cam200usb) was used to measure this characteristic at room temperature. The mean size of the deposited distilled water droplets on the surface of the samples was approximately (10.0 ± 0.2 µL). The average values together with their standard deviations were reported considering more than 10 readings for each ENM.

The thickness (δ) of the prepared ENMs was measured at different points of each sample by employing a micrometer equipped with a probe (ISL Isocontrol) and carrying out at least 50 measurements on three different samples, and finally, the mean value of the thickness together with its corresponding standard deviation was reported.

The *LEP* measurements were performed using distilled water and 30 g/L aqueous NaCl solution for each ENM, considering an effective area of 12.56×10^{-4} m^2. Each sample was placed in a stainless-steel static cell connected to a vessel filled with 2 L of a liquid sample. Then, a constant pressure of approximately 4 kPa was applied over the membrane by means of a nitrogen bottle for 5 min at room temperature. Subsequently, the applied pressure was gradually increased every 2 min with steps of 2 kPa. The registered *LEP* was the applied pressure at which the penetrating liquid across the inter-fiber space was visualized at the bottom of the membrane cell. Finally, we report the average *LEP* value together with its standard deviation considering three different samples for each ENM.

The porosity (ε) was determined based on the density obtained using a Pycnometer: Firstly, by using isopropyl alcohol (IPA) as a penetrating liquid in the inter-fiber space to obtain the polymeric material density. Secondly, by using distilled water as a non-penetrating liquid in the inter-fiber space to obtain the ENM matrix density (ρ_m).

To determine the mean inter-fiber space size (d_i) and its distribution, POROFIL125 was used as the liquid wetting agent and a gas-liquid displacement capillary flow porometer (CFP; POROLUX™ 100, IB-FT Germany). Pressurized air was used as the inert gas for all measurements, and the applied hydrostatic pressure varied from 0 to 1.5 MPa at room temperature (~24°C). ENM samples of 18.5 mm diameter were first wetted and mounted in the sample holder of the porometer. Next, the pressurized air was allowed to flow through the sample in a stepwise manner at 80 s/bar. For each ENM, at least three tests were performed with three different samples for each ENM, and the inter-fiber space was reported together with its standard deviation. More details of the followed procedure was described elsewhere [39, 62].

DCMD tests were carried out for all ENMs using the Lewis cell setup schematized in Figure S1. The Lewis cell consists of two stainless steel jacketed chambers, having a length of 20.5 cm each, and a PVC support placed between the two chambers where Viton O-rings fix the membrane to guarantee the absence of any possible water leakage. The two chambers, feed and permeate, are respectively connected to a thermostat and a chiller through their corresponding water jackets to establish the required temperatures for the DCMD experiments. The thermostat (Techne, model TE-8D) was used to adjust the feed temperature, while the cooling system (Polysciences, model 6206T) was used to adjust the permeate temperature. To guarantee uniform bulk temperatures and concentrations in each chamber, both feed and permeate were stirred by a set of chain-driven magnetic stirrers. A pair of thermocouples (Pt 100) placed near both sides of the membrane surface and connected to a digital meter with an

accuracy of ± 0.1°C were used for temperature measurements. Both the feed and permeate tanks were placed at the same level to eliminate any transmembrane hydrostatic pressure.

The DCMD experiments were conducted first using distilled water as feed and then 35 g/L NaCl aqueous solution as feed while the permeate was distilled water maintaining the stirring speed of in both the feed and permeate chambers fixed at 500 rpm. For leakage testing, permeate flux reproducibility, and wetting or fouling quantification, a DCMD checking experiment was performed before and after each desalination experiment for 5 h, using distilled water as feed (at 70 °C) and in the permeate side (at 20 °C). In each case, the permeate flux (J_w) was calculated by means of Eq. (1), considering the collected condensate in the permeate chamber over a predetermined time. The NaCl concentration of the permeate and feed solutions was determined by measuring the electrical conductivity using a conductivity meter (712 ΩMetrohm), and the salt rejection factor (α) was calculated by Eq. (2):

$$J_w = \frac{m_{permeate}}{A.\Delta t} \quad (1)$$

$$\alpha(\%) = \left(1 - \frac{C_{p,final}}{\frac{C_{f,initial} + C_{f,final}}{2}}\right).100 \quad (2)$$

where $m_{permeate}$ is the weight of the collected permeate over a predetermined time (t), A is the effective membrane area; $C_{f,inicial}$, $C_{f,final}$ and $C_{p,final}$ are the initial and final NaCl concentrations of the feed and permeate solutions, respectively.

3. Results and discussion

3.1 Morphology and hydrophobicity of the prepared ENMs

Natural organic alternatives instead of organic derivatives for promoting the hydrophobicity of MD membranes are attractive choices to be considered. In this study, attempts are made to use Lycopodium spore particles, yet their size is much larger than most organic particles commonly considered in MD membrane modification, as shown in Fig. 1. It can be observed that the Lycopodium particles size is around 27 μm in diameter, are reasonably monodisperse, and exhibit a rough surface. However, its surface shows a distinctive honeycomb structure with an average pore size of 5 μm. The particle size analysis by ImageJ software showed that the diameter of the particles ranged from 20 to 36 μm. Moreover, all Lycopodium particles exhibit the same decoration structure and roughly the same size, evidenced by their narrow size distribution (Fig. 1). As can be seen in Fig. 1, Lycopodium spores are characterized by a spherical head with a honeycomb pattern and possess a Y-shaped marking at the bottom originated by the cell division process during which the spore contacts three other spores arranged in a tetrahedral order, giving them the name of trilete spores [63].

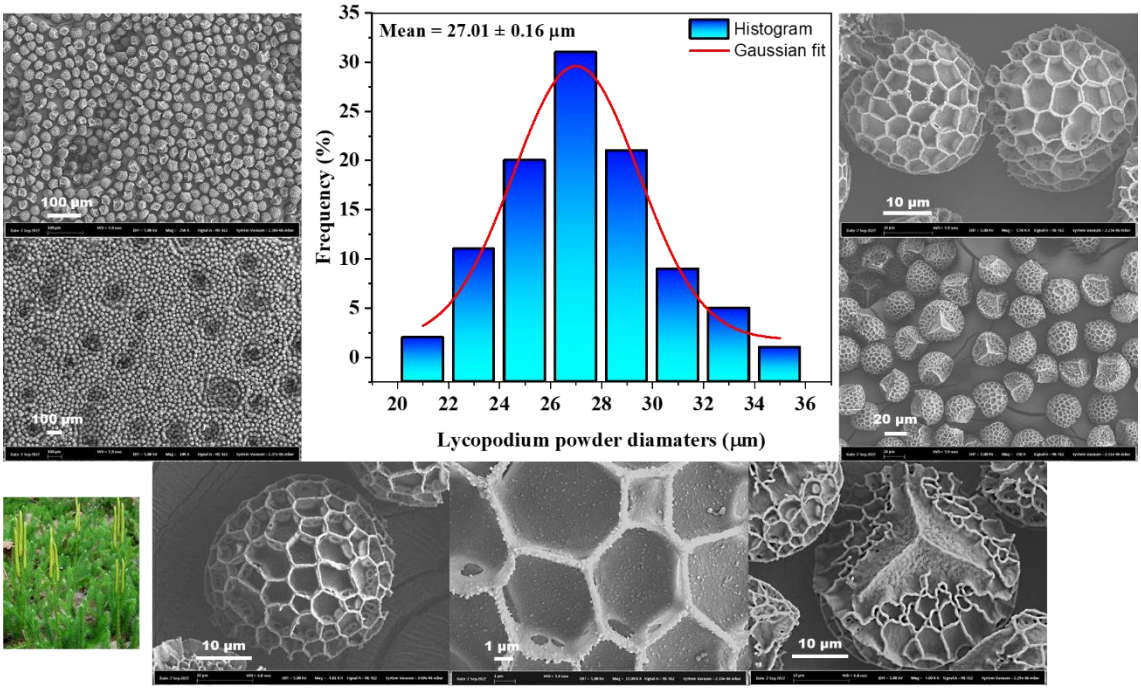

Figure 1. SEM image of the original *Lycopodium clavatum* spore grain at different magnifications shows the details of its morphological structure and size distribution.

As can be seen in Fig. 2 showing the FESEM images of the top surface of the prepared ENMs together with the nanofiber size (d_f) distribution, all PVDF-ENMs-Lyc are composed of randomly oriented nanofibers and Lycopodium beads, which are most likely originated by electrospinning of PVDF and electrospraying of Lycopodium particles. Visibly, the apparent density of Lycopodium particles at the surface of PVDF-ENMs-Lyc increased from 756 to 3465 particles/mm^2 as the Lycopodium content was increased from 0.25 to 3 wt%, indicating an enhancement of 358.33%. Furthermore, Lycopodium-based ENMs surfaces exhibited different textural aspects resulting from the presence of Lycopodium, such as agglomerations and entangled Lycopodium particles within nanofibers and misalignment of nanofibers as indicated with the blue and red circles in Fig 2.

The properties of the polymer solution for electrospinning (especially its surface tension, viscosity, and electrical conductivity) strongly determine the ENMs' morphological structure, particularly their fibers size and beads formation [64]. A decrease of the nanofiber size (d_f) was

observed with the increase of the Lycopodium content in the dope solution (i.e., 50.4% with the increase of Lycopodium concentration from 0 to 3 wt%). A higher Lycopodium content in the PVDF solution resulted in an enhanced electrical conductivity (i.e. an increase of 30.25% when the Lycopodium concentration was 3 wt% compared to that of the PVDF solution, see Table 1), promoting therefore nanofibers with smaller size, regardless of the increase of the viscosity of the polymer solution upon Lycopodium addition. This result indicates the predominant effect of the electrical conductivity on the size of the electrospun nanofibers compared to those of the viscosity and surface tension. The polymeric solution's enhanced electrical conductivity increases the solution jet's surface charge density, causing its elongation and stretching through the air gap as a response to the applied electric field [65, 66]. In addition, Fig. 2 shows relatively more intertwined nanofibers with beads and Lycopodium particles with increasing the Lycopodium content in the electrospinning dope. This can be attributed to the increased surface tension of the polymeric solution with the increase of the Lycopodium concentration (Table 1) [64].

$C_{Lycopodium}$ (wt%)	SEM images		d_f distribution
0.00	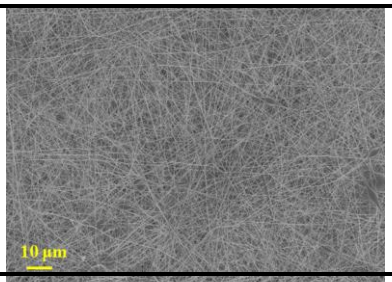	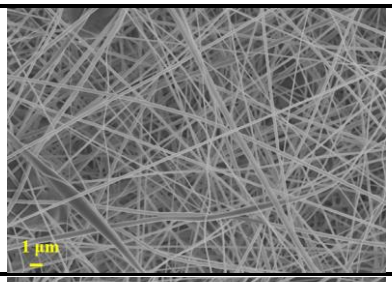	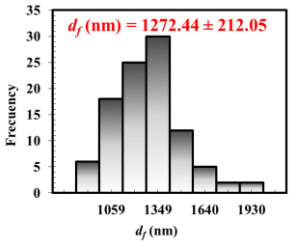
0.25	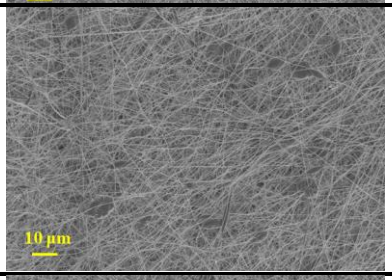	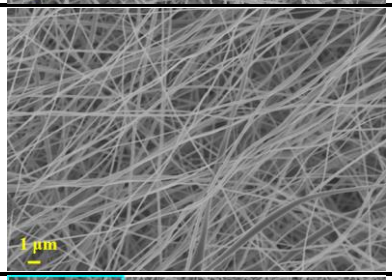	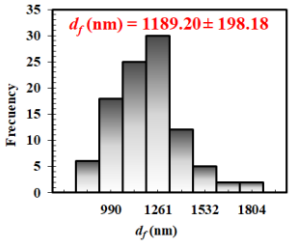
0.50	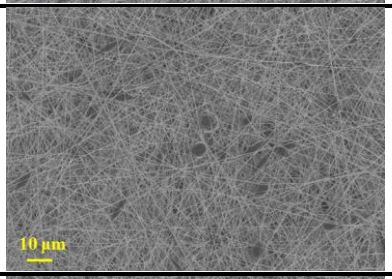	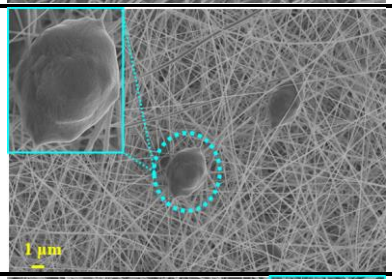	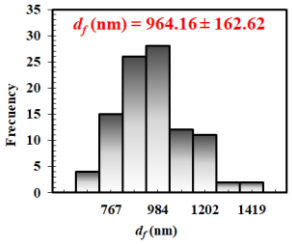
1.00	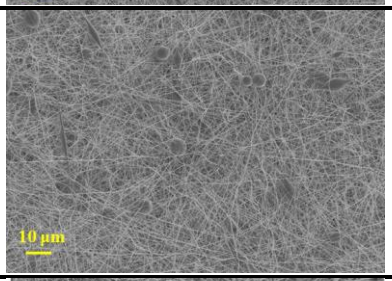	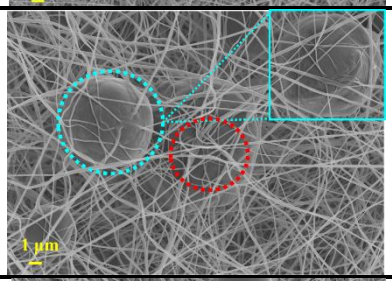	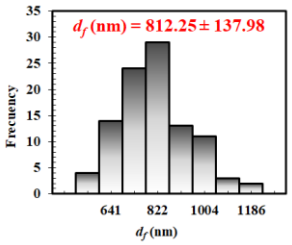
2.00	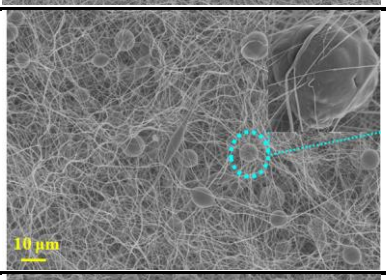	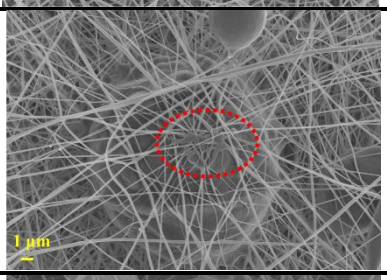	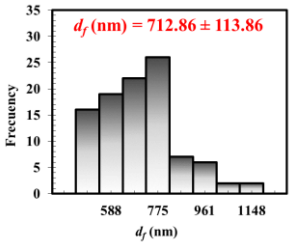
3.00	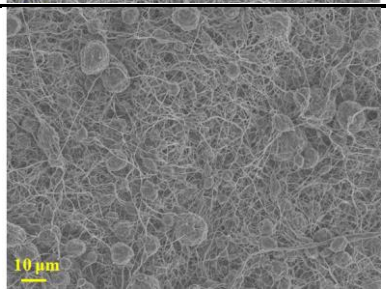	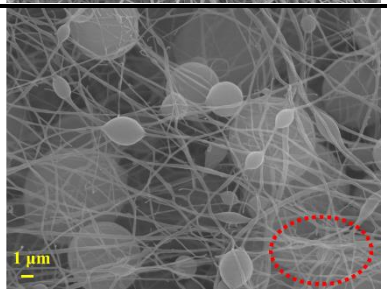	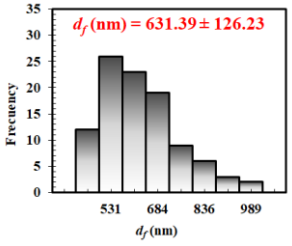

Figure 2. FESEM images of PVDF ENM and PVDF-ENMs-Lyc surfaces prepared with different Lycopodium contents together with histograms showing their nanofiber diameter (d_f) distributions.

For the stable performance of a membrane during the MD process, a strong hydrophobicity of the membrane surface facing the hot feed solution is essential. The surface morphology of PVDF-Lyc-ENM prepared with different Lycopodium contents showed the presence of several beads entangled with fibers of different sizes (i.e., Lycopodium powder particles), showing a roughness at the micro and nanoscale that could potentially increase the surface water contact angles [67-69].

Wettability is recognized as one of the most critical properties of nanofibrous membranes for fundamental and practical applications such as MD. In general, the improvement of hydrophobicity reduces wettability during the MD process. Besides the membrane pore size, this can be controlled by the water contact angle following Young-Laplace equation [70].

Figure 4 shows the enhancement of the water contact angle with the increase of the Lycopodium content. The water droplets deposited on the Lycopodium-based ENM surfaces showed higher apparent contact angle values over 145° than that of PVDF ENM due to the incorporation of Lycopodium in the prepared ENMs. Surprisingly, at Lycopodium content of 1 wt%, ENMs switched to superhydrophobic character, achieving a value of 150.8º and by further increasing Lycopodium content to 3 wt%, the superhydrophobicity of ENMs achieved a value of 161.6º.

According to Cassie et al. studies [53, 71], air can be trapped under the water droplet after its contact with the ENM rough surfaces, forming "air pockets". Consequently, the rough grooves, Lycopodium particles in our case, and the entrapment of air bubbles within the grooves below the water droplet prevent wetting and complete penetration of water, a phenomenon commonly described by the Cassie-Baxter model, which is referred to as the homogeneous

wetting regime [54, 72, 73]. Moreover, due to the particular effect of the Lycopodium particle shape on the increase in surface roughness, the water droplets act as a non-wetting Cassie-Baxter mode rather than a Wenzel mode in such a singular geometry (see Fig. 3).

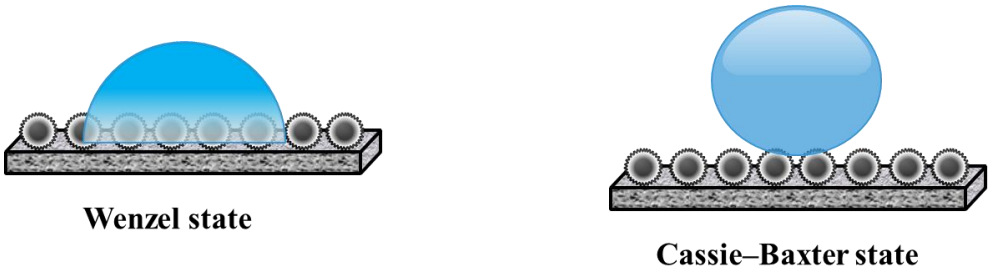

Figure 3. Schematic illustration of Wenzel and Cassie–Baxter contact modes.

Generally speaking, the rough morphological structure and the high hydrophobicity resulting from the presence of Lycopodium in ENMs support the conclusion that incorporating Lycopodium-based particles into polymeric solutions is an effective approach to improve the hydrophobic character of ENMs inducing even superhydrophobicity.

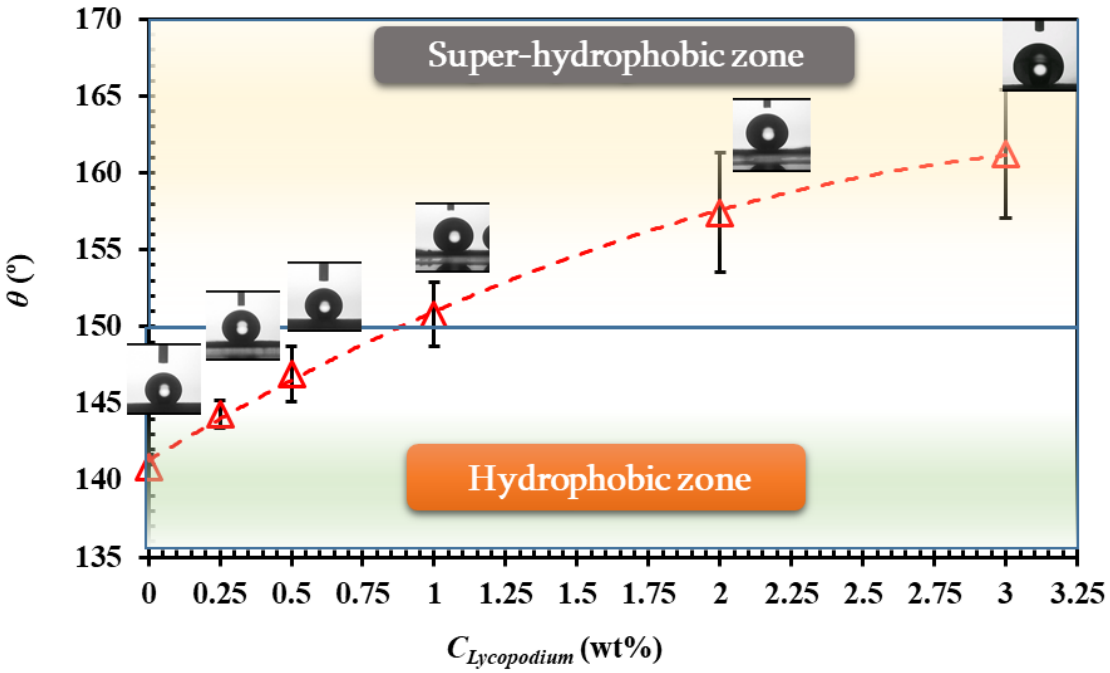

Figure 4. Effect of Lycopodium content ($C_{Lycopodium}$) on water contact angle (θ) of the PVDF-ENMs-Lyc surface and the recorded images of the deposited water droplets.

The void volume fraction (ε), thickness (δ), *LEP*, average inter-fiber space size (d_i), and its distribution are also critical parameters to be known for a good MD performance. Figure 5 shows the change of these parameters with the considered Lycopodium content in the electrospinning PVDF solution.

The void volume fraction of the PVDF ENMs decreased from 0.97 to 0.87 (i.e., a reduction of 10.15%, Fig. 5a) as the Lycopodium content was increased from 0 up to 3 wt%. Meanwhile, the thickness of the ENMs was also increased by 47.59% (Fig. 5a). This can be related to both the increase of the Lycopodium particle density and the gradual increase of the surface tension of the polymeric solution, which enhances the size and density of the beads. Moreover, it must be pointed out that the increase of the Lycopodium content enhances the electrical conductivity of the polymeric solution, leading to a high dissipation of the electrical charges to the metallic collector and less accumulation of charges in the formed nanofibers. This latter effect weakens the possible repulsive interactions between nanofibers and, consequently, promotes the formation of more tightly compacted nanofibrous networks with low void volume fraction values.

It was expected that decreasing the diameter of the nanofiber might result in thinner PVDF-ENMs-Lyc when maintaining the same electrospinning time. However, the thickness of the PVDF-ENMs-Lyc was increased by 47.6% when the amount of Lycopodium reached 3 wt%. This can be attributed partly to the increase of the Lycopodium particles density in the nanofibrous network of PVDF-ENMs-Lyc favoring the formation of thicker nanofibrous membranes regardless of the decrease in nanofiber size.

During ENM formation, the nanofibrous layer formed on the metallic support acts as an electrical insulator, reducing the dissipation of the electric charges to the collector, and favoring therefore their accumulation in the nanofibers and the subsequent repulsive forces between

them that result finally in a less compact nanofiber network. However, the electric charges will dissipate more easily through an ENM layer with a higher electrical conductivity, reducing therefore, their accumulation in the nanofibers and, subsequently, the fibers' repulsion, promoting finally a tightly packed ENM structure. In the present study, for mixed matrix nanofibers, the higher Lycopodium concentration in the dope resulted in a higher electrical conductivity and thicker PVDF-ENMs-Lyc membranes with lower void volume fraction, indicating once again the predominant effect of the electrical conductivity. It is to be noted that the PVDF-ENMs-Lyc prepared in the present study exhibit void volume fraction values similar to those of other types of ENMs [74-77], but greater than those of most commercial membranes, which are prepared for other purposes rather than for MD (Gelman's TF200, TF450, TF1000; Gore's PTS20, PT20, PT45 made of polytetrafluoroethylene supported by a polypropylene net (44-90%) [78, 79]; Millipore's GVHP, HVHP, GVSP, PV22, PV45 made of PVDF (62-80%) [79-81]), and PVDF flat sheet membranes prepared by phase inversion (26.8-79.6%) commonly used in MD [80].

Compared to the PVDF ENM, an improvement of the *LEP* was detected for the PVDF-ENMs-Lyc using distilled water (i.e., an increase from 41.67 to 75.00 kPa) and 35 g/L NaCl aqueous solution (i.e., from 76.67 to 88.33 kPa) with the increase of Lycopodium content (Fig. 5b). This is attributed to both the increase of the hydrophobic character of the ENMs as discussed previously and the reduction of the maximum inter-fiber space, which follows the same void volume fraction tendency. The values of *LEP* for the saline solution were found to be greater than those for distilled water because of the higher surface tension of saline solution compared to that of distilled water, taking into consideration that in Young-Laplace equation the Laplace pressure is proportional to the liquid surface tension [82]. It is noteworthy to mention that the detected ranges of *LEP* values of PVDF-ENMs-Lyc are comparable to those

reported for other nanofibrous membranes prepared by electrospinning for the MD separation process [11, 83].

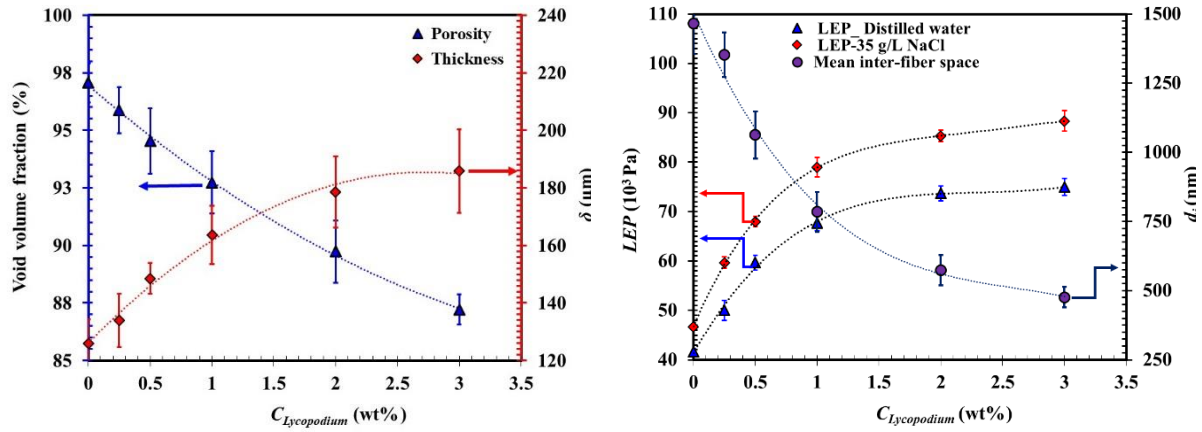

Figure 5. Effects of Lycopodium content on the PVDF ENMs (a) thickness (δ) and the void volume fraction (ε), and (b) the liquid entry pressure (*LEP*) of water and 35 g/L NaCl aqueous solution together with the mean size of the inter-fiber space (d_i).

The inter-fiber space (mean, small, and maximum) of the PVDF-ENMs-Lyc prepared using different Lycopodium content in the PVDF solution together with the inter-fiber space distribution are plotted in Fig. 6a-b. These were obtained using the dry/wet test technique mentioned previously. As shown in both Figs. 5b and 6, a gradual decrease of the inter-fiber space (mean, small, and maximum) was observed with the increase of the Lycopodium concentration in the electrospinning dope solution. A reduction of 69.5% of the mean inter-fiber space could be registered when increasing the Lycopodium content up to 3 wt% (see Fig. 5b, 6a). Moreover, the inter-fiber space distribution curves shifted toward smaller values with increasing Lycopodium content (see Fig. 6b). The same indicated reasoning to explain the void volume fraction tendency is applicable for the inter-fiber space.

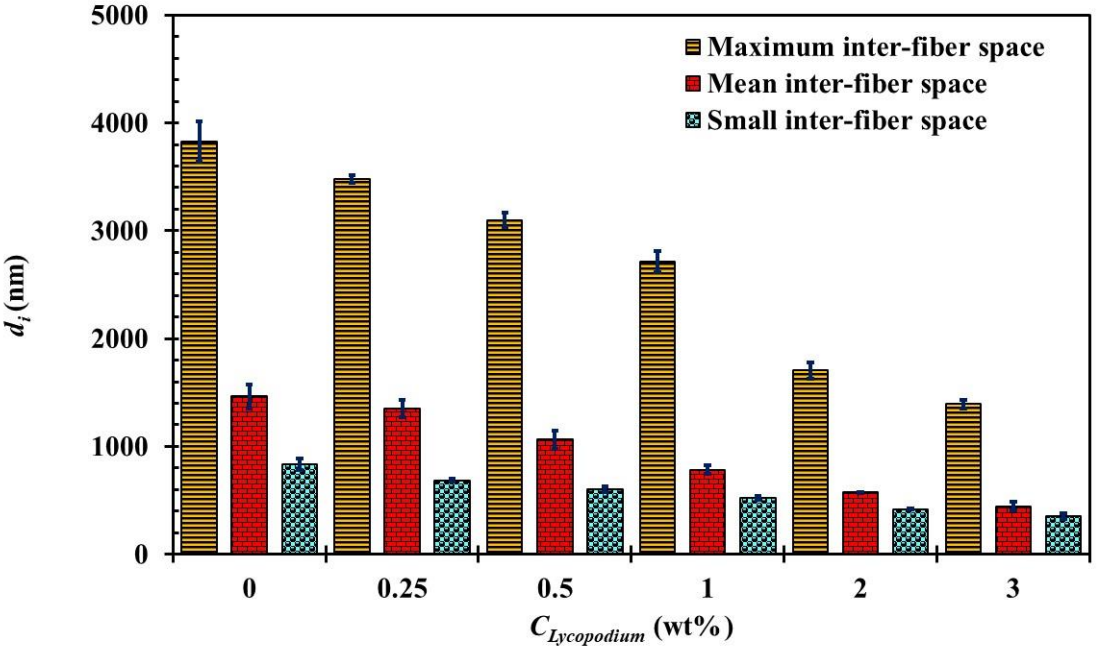

(a)

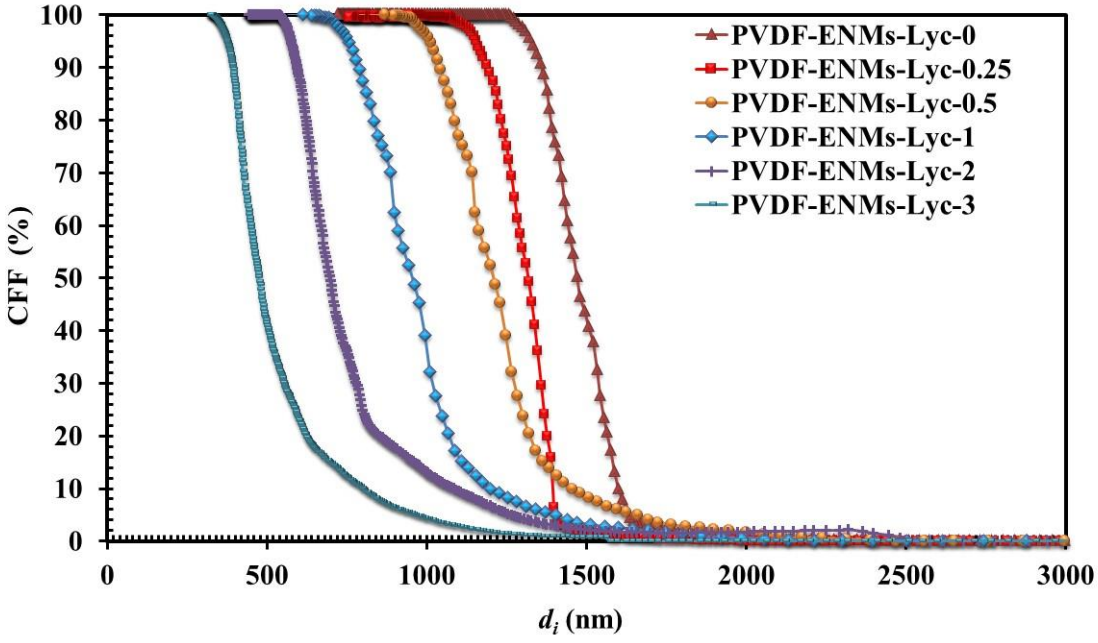

(b)

Figure 6. Variation of the maximum, mean and minimum inter-fiber space (d_i) of the prepared PVDF ENMs with different Lycopodium content (a) and its cumulative distribution (b).

3.2 DCMD performance

Considering the obtained characteristics of the PVDF-ENMs-Lyc, these were tested for desalination by DCMD as described previously. First, the feed temperature (40 to 80 °C) effect on the DCMD of all prepared PVDF ENMs was studied using both distilled water and 35 g/L NaCl aqueous solution as feed, maintaining the permeate temperature at 20 °C. The results are shown in Table S1. As it was expected, it was observed an exponential enhancement of the DCMD permeate flux with increasing the feed temperature for all PVDF ENMs due mainly to the increase of the vapor pressure at the feed/ENM interface following an Arrhenius-type dependence [11, 61]. This is a common behavior of all MD membranes. With the increase of the feed temperature from 40ºC to 80ºC, DCMD permeate flux increased from 40.57 to 57.02 kg/m^2·h for PVDF-ENM-Lyc-3 and from 48.04 to 70.43 kg/m^2·h for PVDF-ENM with increasing the feed temperature from 40 to 80 ºC, respectively. As can be seen in Fig. 7a the permeate flux decreased as the Lycopodium content in the dope solution was increased, and it seems attending asymptotic values for both distilled water and 35 g/L NaCl aqueous solution used as feed. Such reduction of the DCMD permeates flux agrees with the obtained characteristics of the PVDF-ENMs-Lyc, considering that the higher content of Lycopodium in the dope, resulted in thicker ENMs with smaller void volume fraction and inter-fiber space (see Fig. 5a,b). It is well known that in MD, the permeate flux is proportional to the membrane void volume fraction and pore size and is inversely proportional to the membrane thickness [5, 84]. In addition, all PVDF-ENMs-Lyc the permeate flux for the 35 g/L NaCl aqueous solution was found to be smaller than that of distilled water used as feed, and the difference between them became greater for higher temperatures. This is due to the reduction of the vapor pressure of the aqueous feed solution with the increase of the salt concentration and to the concentration polarization effect at the feed/ENM side coupled to the temperature polarization effect already present when distilled water is used as feed [61, 85, 86]. It must be pointed out that the PVDF

ENM prepared without Lycopodium showed lower salt rejection factor (i.e. lower than 99.92% at 40 ºC and 99.86% at 80 ºC; as its final permeate electrical conductivity significantly increased from 3.48 µS/cm to 105.54 µS/cm at 40 °C and from 3.84 µS/cm to 171.34 µS/cm at 80 °C, respectively; Fig. 7b) indicating wetting of this ENM inter-fiber space as its *LEP* is smaller than that of the PVDF-ENMs-Lyc (Fig. 5b). In contrast, the salt rejection factors of all PVDF-ENMs-Lyc were generally over 99.94%, irrespective of the considered feed temperature and Lycopodium content. Compared to the PVDF ENM, the PVDF-ENM-Lyc-0.25 electrospun with 0.25 wt% Lycopodium in the dope showed a slight improvement of the salt rejection factor reflected by a smaller final electrical conductivity of the permeate (i.e. 74.32 µS/cm at 40 ºC and 99.94 µS/cm at 80 ºC starting with an initial value of around 3.84 µS/cm, respectively; See Fig. 7b and Table S1). Again, this increase of the final electrical conductivity of the permeate is attributed to the lower *LEP* value of the PVDF-ENM-Lyc-0.25 compared to the other PVDF-ENMs-Lyc resulting in a partial inter-fiber space wetting caused by the large inter-fiber space (see Fig. 5b and 6).

When increasing the Lycopodium content to 3 wt%, the resulting PVDF-ENM-Lyc-3 exhibited an improved permeate quality with a final electrical conductivity of only 7.40 µS/cm at a feed temperature of 40 ºC and 3.94 µS/cm at 80 ºC starting with an initial permeate electrical conductivity of 3.84 µS/cm (See Fig. 7b and Table S1). This result is due to the high *LEP* achieved for this ENM associated with its superhydrophobic character and low maximum inter-fiber space, as discussed previously (Figs. 4, 5b, 6). Based on the good DCMD performance obtained for this ENM prepared with 3 wt% Lycopodium in the dope solution, a permeate flux of 51.76 kg/m^2.h and a salt rejection factor of 99.998% with a final permeate of 3.94 µS/cm for 35 g/L NaCl aqueous feed solution at 80 °C, this ENM was selected for the following long-term DCMD tests.

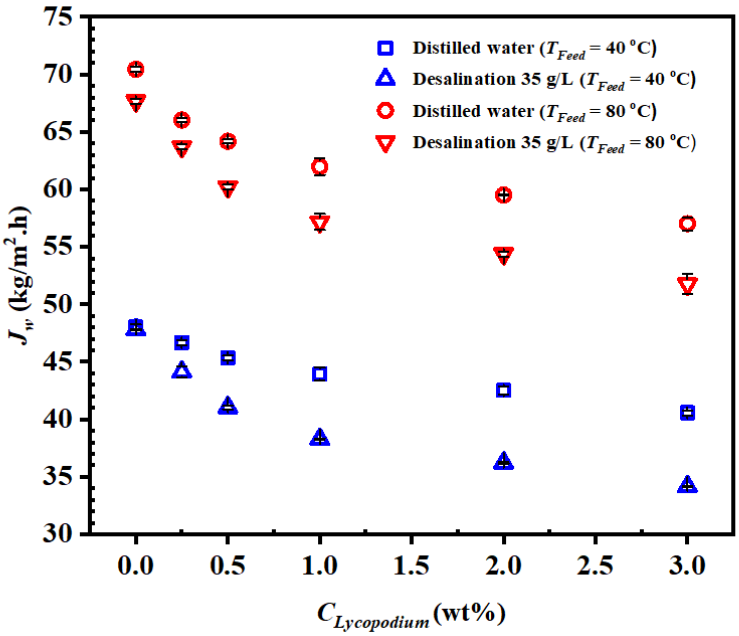

(a)

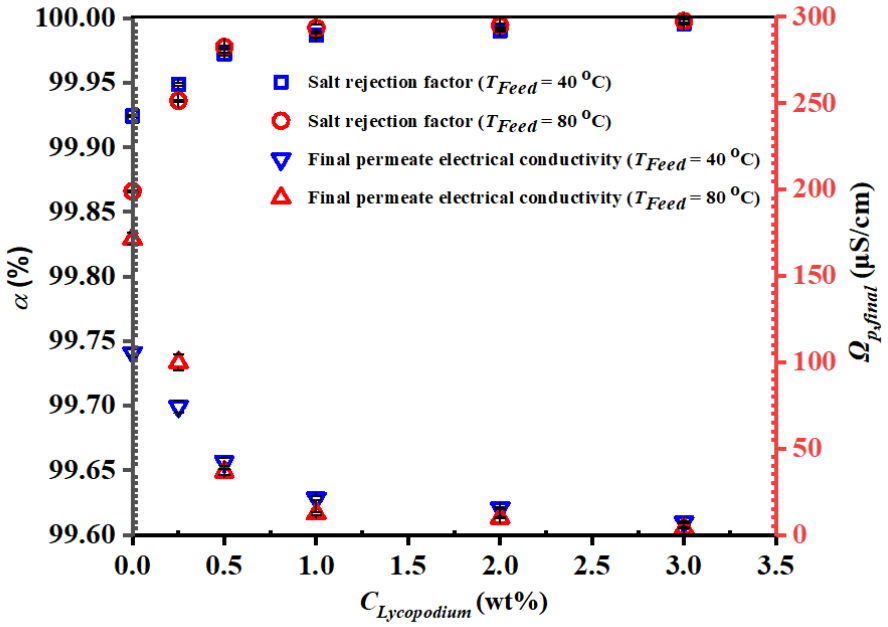

(b)

Figure 7. Effects of Lycopodium content in the dope solution ($C_{Lycopodium}$) and feed temperature (T_f) on the DCMD permeate flux (J_w) using distilled water and 35 g/L NaCl aqueous solution as feed (a), and on the salt rejection factor (α) together with the final permeate electrical conductivity ($\Omega_{p,\text{final}}$) (b), being the initial permeate electrical conductivity ($\Omega_{p,\text{inital}}$) around

3.484 ± 0.523 μS/cm, the permeate temperature (T_p) 20 °C, and the stirring rate of both the feed and permeate solutions 500 rpm.

To test the DCMD stability of the PVDF-ENM-Lyc- 3, DCMD desalination was carried out for 25 h at 80ºC feed temperature and 20ºC permeate temperature using an initial 35 g/L NaCl feed aqueous solution. The permeate flux, salt rejection factor, and final electrical conductivity of the permeate are plotted as a function of the DCMD operating time in Fig. 8. For the sake of comparison only, the PVDF-ENM prepared without Lycopodium was used under the same DCMD conditions, although it was observed that this membrane is unsuitable for MD.

For the PVDF-ENM, an initial DCMD permeate flux of 67.69 kg/m^2.h was registered. However, as it was expected, the permeate flux was increased gradually during the first 12 h of the DCMD experiment (i.e., an increase of 6%), after which a very high permeate flux of about 140.0 kg/m^2.h was reached (i.e., an increase of 106.8%; Fig. 8a) during the next 13 h of DCMD experiment. As can be seen, the salt rejection factor of this PVDF ENM started to decrease after only 1 h DCMD experiment (i.e., over only 1 h DCMD operation the permeate electrical conductivity increased from 3.48 to 171.3 μS/cm and up to 1181. 3 μS/cm for 25 h DCMD operation, Fig. 8b), reaching a very low value around 92%. These results indicated the inter-fiber space wetting of this ENM, confirming its unsuitability for MD applications. In contrast, the PVDF-ENM-Lyc-3 demonstrated to be robust for MD provided that its permeate flux remained stable around 52.39 ± 0.62 kg/m^2.h, with a very high stable salt separation factor of around 99.998 ± 002%. Moreover, as can be seen in Fig.8b, the electrical conductivity of the permeate was maintained very low, less than 6 μs/cm (i.e., in the range 4.003-5.515 μS/cm) with an average value of 4.76 ± 0.46 μS/cm. As stated previously, compared to the other ENMs, this result is attributed to the superhydrophobic character, smaller maximum inter-fiber space, and higher *LEP* of the PVDF-ENM-Lyc-3.

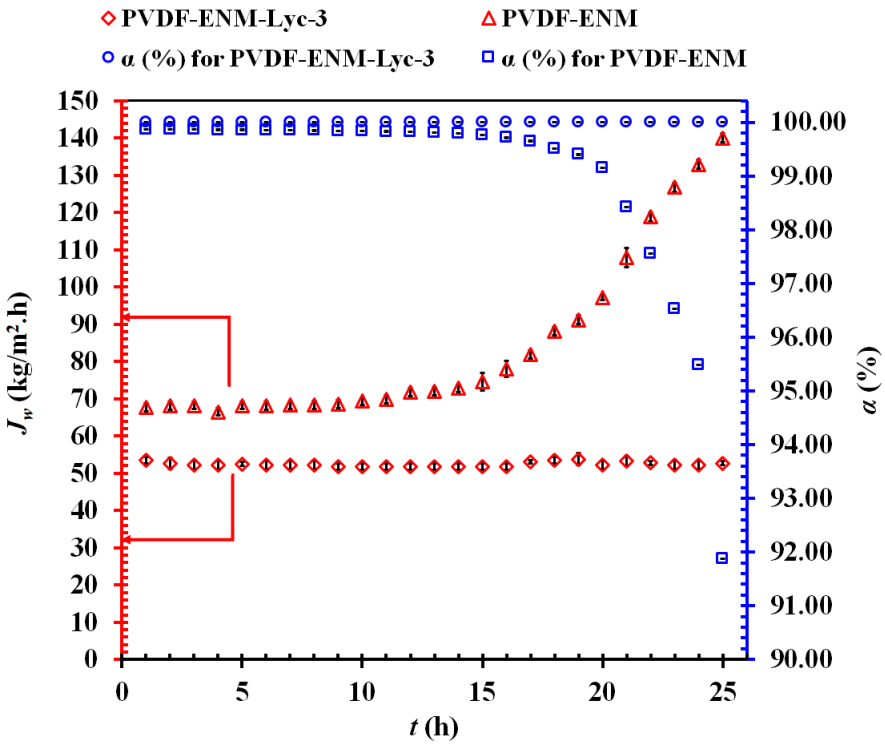

(a)

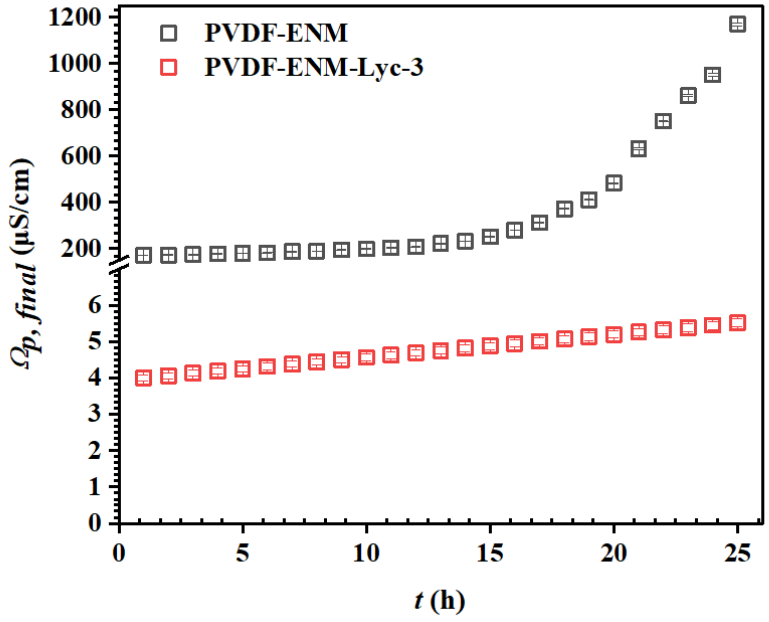

(b)

Figure 8. Permeate flux (J_w) together with the salt rejection factor (α) of both the PVDF-ENM and the PVDF-ENM-Lyc-3 (a) and the permeate electrical conductivity (Ω_p) (b) as a function of the DCMD operating time (t) using initially 35 g/L NaCl aqueous feed solution (T_f = 80 °C, T_p = 20 °C, 500 rpm stirring rate).

At the end of the desalination experiments, the membrane was removed from the module and then subjected to a visual check by visualizing how the water droplets slide over the membrane surface maintaining its superhydrophobic character without showing any sign of wetting or beginning of scaling/fouling (see videos S1 and S2 of the water droplets sliding on the membrane surface before and after DCMD desalination experiments, respectively). This indicates that the tested membrane exhibits a good surface hydrophobic stability with a high potential for desalination. Longer-term desalination experiments than 25 h should be performed using other feed solutions (e.g., wastewater), to investigate whether scaling/fouling occurs or not on this type of membrane.

4. Conclusions

Superhydrophobic electrospun PVDF ENMs with micro- and nanostructured hierarchical surfaces were prepared using a small amount of Lycopodium as a green, inexpensive, biobased additive. The incorporation of Lycopodium particles in PVDF electrospinning solution was found to be an attractive strategy to prepare membranes with superior DCMD desalination performance. Furthermore, more importantly, the structural characteristics of the PVDF ENMs can be adjusted by varying the Lycopodium concentration in the dope solution. The addition of Lycopodium up to 3 wt.% improved significantly the water contact angle up to 161.2º, reduced from 1465 to 476 nm the long-awaited high inter-fiber space of ENMs prepared for MD without heat-pressure post-treatment, enhancing therefore the *LEP* by 89.27 % for the 35 g/L NaCl solution in order to guarantee the stability of the PVDF ENMs. The PVDF ENM prepared with 3 wt% Lycopodium (PVDF-ENM-Lyc-3) yielded the best DCMD performance in terms of the quantity and quality of the produced permeate confirmed by the results of the performed long-term DCMD test (i.e. a stable permeate flux of 52.4 ± 0.6 $kg \cdot m^{-2} \cdot h^{-1}$ with a good salt rejection

factor, 99.998%, and an electrical conductivity around 4.76 ± 0.46 μS/cm when treating 35 g/L NaCl aqueous solution at 80ºC feed temperature and 20ºC permeate temperature).

In general, the results demonstrated that Lycopodium is a viable and environmental-friendly additive for the fabrication of polymeric membranes suitable for MD technology.

References

[1] J. Awange, Global Freshwater Resources, in: J. Awange (Ed.) Food Insecurity & Hydroclimate in Greater Horn of Africa: Potential for Agriculture Amidst Extremes, Springer International Publishing, Cham, 2022, pp. 67-83.

[2] H. Al Maawali, D.J. Kayode Adewole, A. Al Kharusi, J. Al-Qartoubi, M. Al Maamari, R. Al Balushi, R. Al Mazrui, Comparative Studies of Membrane Distillation and Reverse Osmosis for Seawater Desalination, Journal of Student Research, 10 (2021) 1-12.

[3] E.W. Tow, D.M. Warsinger, A.M. Trueworthy, J. Swaminathan, G.P. Thiel, S.M. Zubair, A.S. Myerson, J.H. Lienhard V, Comparison of fouling propensity between reverse osmosis, forward osmosis, and membrane distillation, Journal of Membrane Science, 556 (2018) 352-364.

[4] P.S. Goh, K.C. Wong, A.F. Ismail, Membrane technology: A versatile tool for saline wastewater treatment and resource recovery, Desalination, 521 (2022) 115377.

[5] M. Khayet, A.O. Imdakm, T. Matsuura, Monte Carlo simulation and experimental heat and mass transfer in direct contact membrane distillation, International Journal of Heat and Mass Transfer, 53 (2010) 1249-1259.

[6] B.L. Pangarkar, M.G. Sane, M. Guddad, Reverse Osmosis and Membrane Distillation for Desalination of Groundwater: A Review, ISRN Materials Science, 2011 (2011) 523124.

[7] M. Micari, F. Giacalone, A. Cipollina, G. Micale, A. Tamburini, Chapter 4 - Reverse electrodialysis heat engine (REDHE), in: A. Tamburini, A. Cipollina, G. Micale (Eds.) Salinity Gradient Heat Engines, Woodhead Publishing, 2022, pp. 127-162.

[8] P. Palenzuela, M. Micari, B. Ortega-Delgado, F. Giacalone, G. Zaragoza, D.-C. Alarcón-Padilla, A. Cipollina, A. Tamburini, G. Micale, Performance Analysis of a RED-MED Salinity Gradient Heat Engine, Energies, 11 (2018) 3385.

[9] N. Hilal, A.F. Ismail, C. Wright, Membrane fabrication, CRC Press, 2015.

[10] M. Essalhi, N. Ismail, S. Tesfalidet, J. Pan, Q. Wang, Z. Cui, M.C. García-Payo, M. Khayet, J.-P. Mikkola, S. Sarmad, D. Bouyer, Y. Zhao, B. Li, C. André Ohlin, N. Tavajohi, Polyvinylidene fluoride membrane formation using carbon dioxide as a non-solvent additive for nuclear wastewater decontamination, Chemical Engineering Journal, 446 (2022) 137300.

[11] L. Francis, F.E. Ahmed, N. Hilal, Electrospun membranes for membrane distillation: The state of play and recent advances, Desalination, 526 (2022) 115511.

[12] A.M. Al-Dhahebi, J. Ling, S.G. Krishnan, M. Yousefzadeh, N.K. Elumalai, M.S.M. Saheed, S. Ramakrishna, R. Jose, Electrospinning research and products: The road and the way forward, Applied Physics Reviews, 9 (2022) 011319.

[13] A.A. Puranik, L.N. Rodrigues, J. Chau, L. Li, K.K. Sirkar, Porous hydrophobic-hydrophilic composite membranes for direct contact membrane distillation, Journal of Membrane Science, 591 (2019) 117225.

[14] M. Bhadra, S. Roy, S. Mitra, Flux enhancement in direct contact membrane distillation by implementing carbon nanotube immobilized PTFE membrane, Separation and Purification Technology, 161 (2016) 136-143.

[15] Y.C. Woo, M. Yao, W.-G. Shim, Y. Kim, L.D. Tijing, B. Jung, S.-H. Kim, H.K. Shon, Co-axially electrospun superhydrophobic nanofiber membranes with 3D-hierarchically structured

surface for desalination by long-term membrane distillation, Journal of Membrane Science, 623 (2021) 119028.

[16] Y. Liao, R. Wang, A.G. Fane, Fabrication of Bioinspired Composite Nanofiber Membranes with Robust Superhydrophobicity for Direct Contact Membrane Distillation, Environmental Science & Technology, 48 (2014) 6335-6341.

[17] P. Yadav, R. Farnood, V. Kumar, Superhydrophobic modification of electrospun nanofibrous Si@PVDF membranes for desalination application in vacuum membrane distillation, Chemosphere, 287 (2022) 132092.

[18] A.A. Ali, G.C. Rutledge, Hot-pressed electrospun PAN nano fibers: An idea for flexible carbon mat, Journal of Materials Processing Technology, 209 (2009) 4617-4620.

[19] A.A. Ali, A.R. Eldesouky, S.H. Zoalfakar, Hot-pressed electrospun mwcnts/carbon nano fibril composites: potential applications for breaking pads and journal bearing, The International Conference on Applied Mechanics and Mechanical Engineering, 16 (2014) 1-14.

[20] H. Na, Y. Zhao, C. Zhao, C. Zhao, X. Yuan, Effect of hot-press on electrospun poly(vinylidene fluoride) membranes, Polymer Engineering & Science, 48 (2008) 934-940.

[21] S.P. Muduli, S. Parida, S.K. Rout, S. Rajput, M. Kar, Effect of hot press temperature on β-phase, dielectric and ferroelectric properties of solvent casted Poly(vinyledene fluoride) films, Materials Research Express, 6 (2019) 095306.

[22] M. Yao, Y.C. Woo, L.D. Tijing, W.-G. Shim, J.-S. Choi, S.-H. Kim, H.K. Shon, Effect of heat-press conditions on electrospun membranes for desalination by direct contact membrane distillation, Desalination, 378 (2016) 80-91.

[23] E.I. El-Aswar, H. Ramadan, H. Elkik, A.G. Taha, A comprehensive review on preparation, functionalization and recent applications of nanofiber membranes in wastewater treatment, Journal of Environmental Management, 301 (2022) 113908.

[24] Kenry, C.T. Lim, Nanofiber technology: current status and emerging developments, Progress in Polymer Science, 70 (2017) 1-17.

[25] S.K. Patel, C.L. Ritt, A. Deshmukh, Z. Wang, M. Qin, R. Epsztein, M. Elimelech, The relative insignificance of advanced materials in enhancing the energy efficiency of desalination technologies, Energy & Environmental Science, 13 (2020) 1694-1710.

[26] I. Zucker, N. Dizge, C.L. Fausey, E. Shaulsky, M. Sun, M. Elimelech, Electrospun silica nanofiber mats functionalized with ceria nanoparticles for water decontamination, RSC Advances, 9 (2019) 19408-19417.

[27] Y. Xu, Y. Yang, X. Fan, Z. Liu, Y. Song, Y. Wang, P. Tao, C. Song, M. Shao, In-situ silica nanoparticle assembly technique to develop an omniphobic membrane for durable membrane distillation, Desalination, 499 (2021) 114832.

[28] J. Lee, C. Boo, W.-H. Ryu, A.D. Taylor, M. Elimelech, Development of Omniphobic Desalination Membranes Using a Charged Electrospun Nanofiber Scaffold, ACS Applied Materials & Interfaces, 8 (2016) 11154-11161.

[29] M.S. Islam, K. Touati, M.S. Rahaman, High Flux and Antifouling Thin-Film Nanocomposite Forward Osmosis Membrane with Ingrained Silica Nanoparticles, ACS ES&T Engineering, 1 (2021) 467-477.

[30] B.J. Deka, J. Guo, N.K. Khanzada, A.K. An, Omniphobic re-entrant PVDF membrane with ZnO nanoparticles composite for desalination of low surface tension oily seawater, Water Research, 165 (2019) 114982.

[31] J. Li, L.-F. Ren, H.S. Zhou, J. Yang, J. Shao, Y. He, Fabrication of superhydrophobic PDTS-ZnO-PVDF membrane and its anti-wetting analysis in direct contact membrane distillation (DCMD) applications, Journal of Membrane Science, 620 (2021) 118924.

[32] X. Li, W. Qing, Y. Wu, S. Shao, L.E. Peng, Y. Yang, P. Wang, F. Liu, C.Y. Tang, Omniphobic Nanofibrous Membrane with Pine-Needle-Like Hierarchical Nanostructures:

Toward Enhanced Performance for Membrane Distillation, ACS Applied Materials & Interfaces, 11 (2019) 47963-47971.

[33] O.V. Otieno, E. Csáki, O. Kéri, L. Simon, I.E. Lukács, K.M. Szécsényi, I.M. Szilágyi, Synthesis of TiO2 nanofibers by electrospinning using water-soluble Ti-precursor, Journal of Thermal Analysis and Calorimetry, 139 (2020) 57-66.

[34] A. Razmjou, E. Arifin, G. Dong, J. Mansouri, V. Chen, Superhydrophobic modification of TiO2 nanocomposite PVDF membranes for applications in membrane distillation, Journal of Membrane Science, 415-416 (2012) 850-863.

[35] J.A. Prince, G. Singh, D. Rana, T. Matsuura, V. Anbharasi, T.S. Shanmugasundaram, Preparation and characterization of highly hydrophobic poly(vinylidene fluoride) – Clay nanocomposite nanofiber membranes (PVDF–clay NNMs) for desalination using direct contact membrane distillation, Journal of Membrane Science, 397-398 (2012) 80-86.

[36] R. Neppalli, S. Wanjale, M. Birajdar, V. Causin, The effect of clay and of electrospinning on the polymorphism, structure and morphology of poly(vinylidene fluoride), European Polymer Journal, 49 (2013) 90-99.

[37] Y.C. Woo, L.D. Tijing, W.-G. Shim, J.-S. Choi, S.-H. Kim, T. He, E. Drioli, H.K. Shon, Water desalination using graphene-enhanced electrospun nanofiber membrane via air gap membrane distillation, Journal of Membrane Science, 520 (2016) 99-110.

[38] A. Kyoungjin An, E.-J. Lee, J. Guo, S. Jeong, J.-G. Lee, N. Ghaffour, Enhanced vapor transport in membrane distillation via functionalized carbon nanotubes anchored into electrospun nanofibres, Scientific Reports, 7 (2017) 41562.

[39] M. Essalhi, M. Khayet, S. Tesfalidet, M. Alsultan, N. Tavajohi, Desalination by direct contact membrane distillation using mixed matrix electrospun nanofibrous membranes with carbon-based nanofillers: A strategic improvement, Chemical Engineering Journal, 426 (2021) 131316.

[40] L.D. Tijing, Y.C. Woo, W.-G. Shim, T. He, J.-S. Choi, S.-H. Kim, H.K. Shon, Superhydrophobic nanofiber membrane containing carbon nanotubes for high-performance direct contact membrane distillation, Journal of Membrane Science, 502 (2016) 158-170.

[41] F. Jahanmard, M. Baghban Eslaminejad, M. Amani-Tehran, F. Zarei, N. Rezaei, M. Croes, S. Amin Yavari, Incorporation of F-MWCNTs into electrospun nanofibers regulates osteogenesis through stiffness and nanotopography, Materials Science and Engineering: C, 106 (2020) 110163.

[42] H. Li, W. Shi, X. Zeng, S. Huang, H. Zhang, X. Qin, Improved desalination properties of hydrophobic GO-incorporated PVDF electrospun nanofibrous composites for vacuum membrane distillation, Separation and Purification Technology, 230 (2020) 115889.

[43] N.F. Himma, N. Prasetya, S. Anisah, I.G. Wenten, Superhydrophobic membrane: progress in preparation and its separation properties, Reviews in Chemical Engineering, 35 (2019) 211-238.

[44] J.A. Prince, D. Rana, G. Singh, T. Matsuura, T. Jun Kai, T.S. Shanmugasundaram, Effect of hydrophobic surface modifying macromolecules on differently produced PVDF membranes for direct contact membrane distillation, Chemical Engineering Journal, 242 (2014) 387-396.

[45] W. Xia, G. Peng, Y. Hu, G. Dou, Desired properties and corresponding improvement measures of electrospun nanofibers for membrane distillation, reinforcement, and self-healing applications, Polymer Engineering & Science, 62 (2022) 247-268.

[46] S.S. Ray, S.-S. Chen, C.-W. Li, N.C. Nguyen, H.T. Nguyen, A comprehensive review: Electrospinning technique for fabrication and surface modification of membranes for water treatment application, RSC advances, 6 (2016) 85495-85514.

[47] S. Santoro, A.H. Avci, A. Politano, E. Curcio, The advent of thermoplasmonic membrane distillation, Chemical Society Reviews, 51 (2022) 6087-6125.

[48] P. Aussillous, D. Quéré, Liquid marbles, Nature, 411 (2001) 924-927.

[49] E. Bormashenko, R. Pogreb, G. Whyman, A. Musin, Y. Bormashenko, Z. Barkay, Shape, vibrations, and effective surface tension of water marbles, Langmuir, 25 (2009) 1893-1896.

[50] E. Bormashenko, R. Grynyov, Plasma treatment allows water suspending of the natural hydrophobic powder (lycopodium), Colloids and Surfaces B: Biointerfaces, 97 (2012) 171-174.

[51] H. Ollivier, Recherches sur la capillarité, J. Phys. Theor. Appl., 6 (1907) 757-782.

[52] R.N. Wenzel, Resistance of solid surfaces to wetting by water, Industrial & Engineering Chemistry, 28 (1936) 988-994.

[53] A. Cassie, S. Baxter, Wettability of porous surfaces, Transactions of the Faraday society, 40 (1944) 546-551.

[54] E. Bormashenko, T. Stein, R. Pogreb, D. Aurbach, "Petal Effect" on Surfaces Based on Lycopodium: High-Stick Surfaces Demonstrating High Apparent Contact Angles, The Journal of Physical Chemistry C, 113 (2009) 5568-5572.

[55] G. McHale, S.J. Elliott, M.I. Newton, D.L. Herbertson, K. Esmer, Levitation-Free Vibrated Droplets: Resonant Oscillations of Liquid Marbles, Langmuir, 25 (2009) 529-533.

[56] E. Pehlivan, M. Ersoz, S. Yildiz, H.J. Duncan, Sorption of Heavy Metal Ions on New Metal-Ligand Complexes Chemically Derived from Lycopodium clavatum, Separation Science and Technology, 29 (1994) 1757-1768.

[57] B.P. Binks, J.H. Clint, G. Mackenzie, C. Simcock, C.P. Whitby, Naturally Occurring Spore Particles at Planar Fluid Interfaces and in Emulsions, Langmuir, 21 (2005) 8161-8167.

[58] A.K.F. Dyab, E.M. Abdallah, S.A. Ahmed, M.M. Rabee, Fabrication and Characterisation of Novel Natural <i>Lycopodium clavatum</i> Sporopollenin Microcapsules Loaded <i>In-Situ</i> with Nano-Magnetic Humic Acid-Metal Complexes, Journal of Encapsulation and Adsorption Sciences, Vol.06No.04 (2016) 23.

[59] A. Diego-Taboada, S.T. Beckett, S.L. Atkin, G. Mackenzie, Hollow pollen shells to enhance drug delivery, Pharmaceutics, 6 (2014) 80-96.

[60] N. Sudareva, O. Suvorova, N. Saprykina, A. Vilesov, P. Bel'tiukov, S. Petunov, A. Radilov, Two-level delivery systems for oral administration of peptides and proteins based on spore capsules of Lycopodium clavatum, Journal of materials chemistry b, 5 (2017) 7711-7720.

[61] M. Khayet, J.I. Mengual, Effect of salt concentration during the treatment of humic acid solutions by membrane distillation, Desalination, 168 (2004) 373-381.

[62] A. Jena, K. Gupta, Characterization of pore structure of filtration media, Fluid/Particle Separation Journal, 14 (2002) 227-241.

[63] G. Shaw, The chemistry of sporopollenin, in: Sporopollenin, Elsevier, 1971, pp. 305-350.

[64] H. Fong, I. Chun, D.H. Reneker, Beaded nanofibers formed during electrospinning, Polymer, 40 (1999) 4585-4592.

[65] C.J. Angammana, S.H. Jayaram, Analysis of the Effects of Solution Conductivity on Electrospinning Process and Fiber Morphology, IEEE Transactions on Industry Applications, 47 (2011) 1109-1117.

[66] R.H. Magarvey, L.E. Outhouse, Note on the break-up of a charged liquid jet, Journal of Fluid Mechanics, 13 (1962) 151-157.

[67] K. Boussu, B. Van der Bruggen, A. Volodin, J. Snauwaert, C. Van Haesendonck, C. Vandecasteele, Roughness and hydrophobicity studies of nanofiltration membranes using different modes of AFM, Journal of colloid and interface science, 286 (2005) 632-638.

[68] N. Nuraje, W.S. Khan, Y. Lei, M. Ceylan, R. Asmatulu, Superhydrophobic electrospun nanofibers, Journal of Materials Chemistry A, 1 (2013) 1929-1946.

[69] S. Li, L. Li, J. Zhong, R. Ma, X. Xu, H. Wu, Y. Yu, Engineering beads-on-string structural electrospun nanofiber Janus membrane with multi-level roughness for membrane distillation, Desalination, 539 (2022) 115950.

[70] R. Di Felice, Liquid Entry Pressure (LEP or LEPW), in: E. Drioli, L. Giorno (Eds.) Encyclopedia of Membranes, Springer Berlin Heidelberg, Berlin, Heidelberg, 2015, pp. 1-1.

[71] A. Cassie, Contact angles, Discussions of the Faraday society, 3 (1948) 11-16.

[72] A. Marmur, Wetting on Hydrophobic Rough Surfaces: To Be Heterogeneous or Not To Be?, Langmuir, 19 (2003) 8343-8348.

[73] A. Marmur, The Lotus Effect: Superhydrophobicity and Metastability, Langmuir, 20 (2004) 3517-3519.

[74] Y. Liao, G. Zheng, J.J. Huang, M. Tian, R. Wang, Development of robust and superhydrophobic membranes to mitigate membrane scaling and fouling in membrane distillation, Journal of Membrane Science, 601 (2020) 117962.

[75] C. Su, Y. Li, H. Cao, C. Lu, Y. Li, J. Chang, F. Duan, Novel PTFE hollow fiber membrane fabricated by emulsion electrospinning and sintering for membrane distillation, Journal of Membrane Science, 583 (2019) 200-208.

[76] Z. Wang, C. Zhao, Z. Pan, Porous bead-on-string poly(lactic acid) fibrous membranes for air filtration, Journal of Colloid and Interface Science, 441 (2015) 121-129.

[77] H. Ke, E. Feldman, P. Guzman, J. Cole, Q. Wei, B. Chu, A. Alkhudhiri, R. Alrasheed, B.S. Hsiao, Electrospun polystyrene nanofibrous membranes for direct contact membrane distillation, Journal of Membrane Science, 515 (2016) 86-97.

[78] M.A. Izquierdo-Gil, M.C. García-Payo, C. Fernández-Pineda, Air gap membrane distillation of sucrose aqueous solutions, Journal of Membrane Science, 155 (1999) 291-307.

[79] M. Khayet, Membranes and theoretical modeling of membrane distillation: A review, Advances in Colloid and Interface Science, 164 (2011) 56-88.

[80] E. Drioli, A. Ali, F. Macedonio, Membrane distillation: Recent developments and perspectives, Desalination, 356 (2015) 56-84.

[81] Direct contact membrane distillation for nuclear desalination. Part I: Review of membranes used in membrane distillation and methods for their characterisation, International Journal of Nuclear Desalination, 1 (2005) 435-449.

[82] H.T. El-Dessouky, H.M. Ettouney, Fundamentals of salt water desalination, Elsevier, 2002.

[83] L. Eykens, K. De Sitter, C. Dotremont, L. Pinoy, B. Van der Bruggen, Membrane synthesis for membrane distillation: A review, Separation and Purification Technology, 182 (2017) 36-51.

[84] M. Essalhi, M. Khayet, Self-sustained webs of polyvinylidene fluoride electrospun nanofibers at different electrospinning times: 1. Desalination by direct contact membrane distillation, Journal of Membrane Science, 433 (2013) 167-179.

[85] M. Suleman, M. Asif, S.A. Jamal, Temperature and concentration polarization in membrane distillation: A technical review, Desalin. Water Treat, 229 (2021) 52-68.

[86] M. Khayet, M.P. Godino, J.I. Mengual, Study of Asymmetric Polarization in Direct Contact Membrane Distillation, Separation Science and Technology, 39 (2005) 125-147.